Phase synchronization of chaotic attractors in the presence of two competing periodic signals

Romulus Breban and Edward Ott*

Institute for Research in Electronics and Applied Physics and Department of Physics, University of Maryland, College Park, Maryland 20742

We discuss the situation where two periodic signals compete to phase synchronize a chaotic attractor. Depending on the relative position of the periods with respect to the synchronization tongue for a single frequency signal, we distinguish several different cases. We find that, depending on parameters, it is possible that one or the other signal will entrain exclusively, or that they will entrain alternately, at their average frequency, or not at all.

I. INTRODUCTION

Phase synchronization of chaos has attracted much attention due to its applicability to a wide range of situations including laser, plasma, fluid, and biological experiments. Synchronization of chaotic attractors with the phase of a periodic externally coupled signal has been studied theoretically [1–5] and demonstrated experimentally [6,7]. Phase synchronization of coupled chaotic systems has also been studied [8–13].

In order to define phase synchronism, assume that we are given two signals a and b where both possess an oscillatory character, such that phases $\phi_a(t)$ and $\phi_b(t)$ can, by some appropriate means, be defined for the two signals. Here the phases $\phi_{a,b}(t)$ are assumed to be continuous in time (i.e., they are not taken modulo 2π), so that, if, for two times $t_2 > t_1$, we have $\phi_{a,b}(t_2) - \phi_{a,b}(t_1) = 2N\pi$, then we say that the phase $\phi_{a,b}$ has executed N counterclockwise rotations between time t_1 and time t_2. (Thus, $\phi_{a,b}$ is defined on the real line rather than on $[0,2\pi]$. This is referred to as the "lift" of the angle.)

Two types of phase synchronism can be distinguished: *strong phase synchronism* and *weak phase synchronism*. In terms of the difference $\Delta\phi(t) = \phi_a(t) - \phi_b(t)$, there is strong phase synchronism between the signals a and b if

$$-K \leq \Delta\phi(t) - \phi_0 \leq K$$

for some constants K and ϕ_0 (typically $K \sim \pi$) and all time t. Thus, $|\Delta\phi|$ does not increase without bound. In weak phase synchronism $|\Delta\phi|$ may become arbitrarily large with increasing time, but the behavior of $\Delta\phi(t)$ as a function of time manifests correlations between the two phases (examples will be given subsequently).

In this paper we consider the case where two periodic signals compete to entrain a chaotic oscillator. There are several possible motivations for this study. First, there may be real situations where a chaotic dynamical system simultaneously receives inputs from two distinct periodic systems (e.g., a neuron receiving signals from two other neurons). Second, the study of a signal with two frequencies can be

regarded as a next step from the single frequency case in obtaining an understanding of phase synchronization of chaos by signals with nontrivial frequency power spectra (Sec. IV). Third, this situation is a generalization of the problem in which two periodic signals compete to entrain a nonlinear *periodic* oscillator.

II. MODEL

We consider a specific model system consisting of a *modified* chaotic Roessler [14] oscillator coupled to a two frequency input signal, $s(t)$. If we denote the regular Roessler system by $d\mathbf{x}/dt = \mathbf{R}(\mathbf{x})$, where $\mathbf{x}^T = [x(t), y(t), z(t)]$, then our modified (undriven) system is [4] $d\mathbf{x}/dt = f(\mathbf{x})\mathbf{R}(\mathbf{x})$, where f is a scalar function of $\mathbf{x}$ that is positive in the region of the chaotic attractor. This modification of the Roessler system does not change the topology of the trajectory curves followed by orbits in phase space, but it does modify the speed with which orbits move along these curves. The motivation for doing this [4] is that the original Roessler system displays a frequency spectrum with a near-δ-function-like feature, corresponding to the average period for an orbit to circulate arround the attractor. This type of behavior is typically not present or expected in the experimental studies [6,7,9–13]. By our modification, we introduce enhanced dispersion in the time for an orbit to circulate around the attractor, and hence the width in the Fourier peak. We take $f(\mathbf{x}) = 1 + \sigma(r^2 - \bar{r}^2)$, $\sigma = 0.002$, $r^2 = x^2 + y^2$, with $\bar{r}$ equal to the time average of τ for the unmodified and unentrained Roessler system ($\bar{r} = 5.037$) [15]. Our model system becomes [4]

$$dx/dt = -[1 + 0.002(r^2 - \bar{r}^2)](y+z),$$

$$dy/dt = [1 + 0.002(r^2 - \bar{r}^2)](x + 0.25y) + s(t), \quad (1)$$

$$dz/dt = [1 + 0.002(r^2 - \bar{r}^2)][0.90 + z(x - 6.0)],$$

where

$$s(t) = A_1 \cos(\omega_1 t) + A_2 \cos(\omega_2 t), \quad (2)$$

and we have chosen the parameters of the Roessler system so that it is in the so-called phase coherent regime (i.e., the x-y projection of the trajectory of the chaotic system with

---

*Also at Department of Electrical and Computer Engineering.
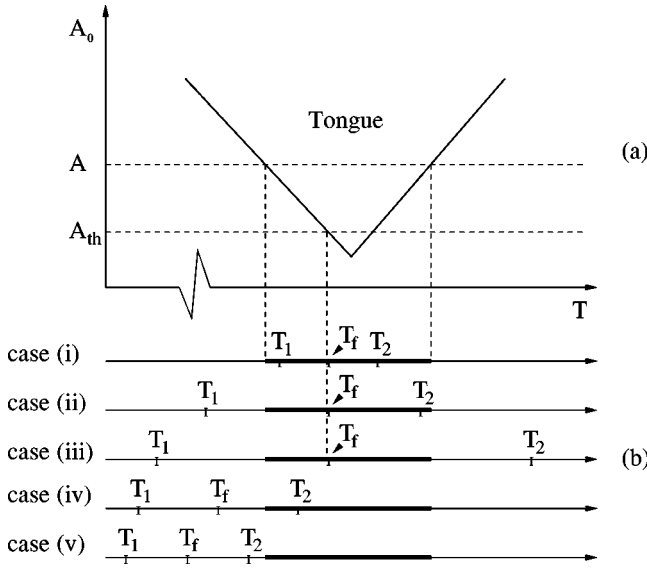
FIG. 1. (a) Schematic representation of the parameter space $A_0 - T$ for the case where there is a single sinusoidal signal, $s(t) = A_0 \cos(2\pi t/T)$, coupled to the Roessler system. (b) Illustration of various cases for the situation in which a signal, consisting of the sum of two equal amplitude sinusoids, $s(t) = A\cos(2\pi t/T_1) + A\cos(2\pi t/T_2)$, is coupled with the Roessler system $[T_1 < T_2, \ T_f = 2T_1T_2/(T_1+T_2)]$. The bold horizontal lines represent the range of T over which phase synchronism occurs for a single sinusoidal signal of amplitude $A_0 = A$.

$A_1 = A_2 = 0$ continually circles around $x = y = 0$, and the x-y projection of the attractor appears to be shaped like an annulus with $x = y = 0$ in the hole of the annulus). Our main goals in this paper are to examine the illustrative system (1),(2) in different regimes, and to delineate and explain the various types of observed phenomena. We conjecture that the phenomena we observe for the system (1),(2) are typical for general oscillatory chaotic systems subject to two frequency external driving.

From studies of the phase synchronism of chaos by a single sinusoidal signal, $s_0(t) = A_0 \sin \omega t$, $\omega = 2\pi/T$, [3,4] it is known that the parameter space given by the amplitude A_0 and period T of the signal typically displays a tongue-shaped region where the phase of the attractor locks with the phase of the periodic signal (i.e., perfect phase synchronism), as shown schematically in Fig. 1(a). For the purpose of the subsequent discussion we also note that the two frequency entraining signal (2) can be written in an alternate form,

$$s(t) = (A_1 + A_2)\cos[(\omega_1 + \omega_2)t/2]\cos[(\omega_1 - \omega_2)t/2]$$

$$+ (A_2 - A_1)\sin[(\omega_1 + \omega_2)t/2]\sin[(\omega_1 - \omega_2)t/2].$$

$$(3)$$

In most of our numerical work we have considered the case of equal amplitudes $A_1 = A_2 = A = 0.06$. (Later we will discuss the case where A_1 and A_2 are different.) From Eq. (3), the entraining signal $s(t)$ can be regarded as a modulated wave, a "fast wave" at the mean frequency
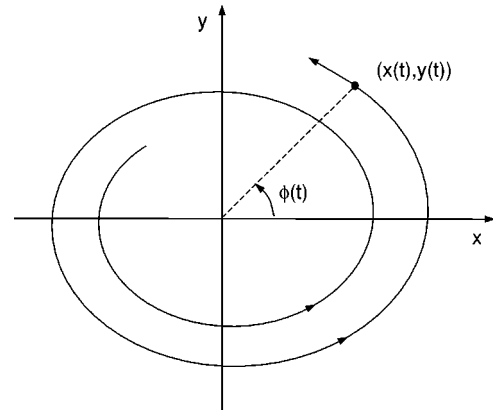
$$\omega_f = (\omega_1 + \omega_2)/2$$

modulated by a "slow wave" at the frequency

$$\omega_s = (\omega_1 - \omega_2)/2,$$

where, for $A_1 = A_2 = A$, the modulating slow wave is

$$\hat{A}(t) = 2A \cos[(\omega_1 - \omega_2)t/2].$$

In our numerical experiments $(\omega_1 + \omega_2) \gg (\omega_1 - \omega_2) > 0$. Three periods will prove relevant: $T_{1,2} = 2\pi/\omega_{1,2}$ and $T_f = 2\pi/\omega_f = 2T_1T_2/(T_1+T_2)$. The geometrical phase of an orbit (Fig. 2) is given by $\tan \phi(t) = [y(t)/x(t)]$ where the relevant branch of $\tan \phi(t) = [y(t)/x(t)]$ is determined by the previously mentioned definition of $\phi(t)$ as continuous in t; see Sec. I. We investigate how $\phi(t)$ is related to the phases of the sinusoidal signals $\phi_{1,2} = \omega_{1,2}t$ as well as to the phase based on the mean frequency $\phi_f = \omega_f t$. As in previous studies, the phase differences,

$$\Delta\phi_{1,2,f}(t) = \phi(t) - \phi_{1,2,f},$$

are used to test phase synchronism between the chaotic orbits of our driven Roessler system (1),(2) and one of the three phases ϕ_1, ϕ_2, or ϕ_f.

We note that synchronism at $\phi_f = \frac{1}{2}(\omega_1 + \omega_2)t$ can be viewed as a special case of the general situation where $l\phi$ synchronizes with $m\phi_1 + n\phi_2$, where l, m, and n are integers. In this framework, synchronism with ϕ_f corresponds to $l = 2$ and $m = n = 1$.

FIG. 2. Graphical illustration of the definition of geometrical phase $\phi(t)$ for a chaotic orbit.

III. RESULTS

We now report and discuss the results of computations for several different choices of the parameters T_1 and T_2. These results serve to illustrate the main qualitative behaviors that we have found. In particular, we consider the five sets of parameter values given in Table I. For each of the parameter sets of Table I the disposition of the values T_1, T_2, and T_f with respect to the tongue of perfect phase synchronism for a single frequency driving signal is illustrated schematically in Fig. 1(b). We first give a detailed account for case (i)

TABLE I. Parameter values T_1 and T_2.

Case	T_1	T_2
(i)	5.95	5.99
(ii)	5.90	5.99
(iii)	5.00	7.40
(iv)	5.00	5.99
(v)	5.00	5.50

followed by brief descriptions of the results for the other cases.

A. Case (i)

In this case there are clear intervals of time, lasting many rotations of ϕ or $\phi_{1,2,f}$ [note that $(\omega_1-\omega_2)/\omega_f \ll 1$], when ϕ is entrained by ϕ_2. In such a time interval, the fluctuation of $\Delta\phi_2/(2\pi)$ is limited to within a narrow range, while

$$\Delta\phi_1/(2\pi) = \Delta\phi_2/(2\pi) - (\omega_1-\omega_2)t/(2\pi)$$

decreases with time at an average rate $(\omega_1-\omega_2)/(2\pi)$. This behavior is seen in Figs. 3(a1) and 3(a2), which show $\Delta\phi_1/(2\pi)$ and $\Delta\phi_2/(2\pi)$ versus $\phi_f/(2\pi) = t/T_f$ over a range representing over 10^4 rotations of ϕ_f. Refering to Fig. 3(a2), plateaus representing locking of ϕ to ϕ_2 are clearly evident and are indicated in the figure by arrowheads (the longest of these plateaus represents approximately 500 rotations of ϕ_f). We also note that each plateau is centered at a value of $\Delta\phi_2/(2\pi)$ that is larger than that for the previous plateau by an integer. That is, ϕ slips relative to ϕ_2 by an integer number of complete rotations between plateaus. [By the arrowheads in Fig. 3(a2) we have considered a plateau to exist if it is at least as wide as $T_s/2 = 2\pi/(\omega_1-\omega_2)$, i.e., half the period of the slow wave.] Referring to Fig. 3(a1), we see that the graph of $\Delta\phi_1/(2\pi)$ versus $\phi_f/(2\pi) = t/T_f$ appears to consist of intervals of approximate linear decrease (with superposed fluctuations) at a slope $-(\omega_1-\omega_2)/\omega_f$ separated by glitches. The intervals of time corresponding to apparent linear decrease of $\Delta\phi_1/(2\pi)$ coincide with the plateaus of $\Delta\phi_2/(2\pi)$, while the glitches in $\Delta\phi_1/(2\pi)$ coincide with the time intervals between the plateaus of $\Delta\phi_2/(2\pi)$. Alternatively, one may consider these glitches to be narrow pla-

teaus of $\Delta\phi_1/(2\pi)$. A close examination of Fig. 3(a1) also shows that the average values of $\Delta\phi_1/(2\pi)$ corresponding to these narrow plateaus differ by integers. ϕ slips relative to ϕ_1 by an integer number of complete rotations between plateaus. Thus in the competition between ϕ_1 and ϕ_2 to entrain ϕ, there are intervals when ϕ_1 wins and intervals when ϕ_2 wins, but, overall, ϕ_2 is a stronger entrainer that ϕ_1. This is also indicated in Figs. 3(a1) and 3(a2) by the fact that, in the same time interval, $\Delta\phi_1$ goes through more than 30 rotations, while $\Delta\phi_2$ only goes through 9. [The relative entraining strengths of ϕ_1 and ϕ_2 depend on the locations of T_1 and T_2 within the tongue in Fig. 1(a).] Figure 4(a) plots $\Delta\phi_1$ versus $\Delta\phi_2$. The staircaselike structure shows that when $\Delta\phi_1$ varies, $\Delta\phi_2$ is approximately constant and vice versa; the approximately horizontal portions of the graph correspond to plateaus of $\Delta\phi_2$ and the approximately vertical portions correspond to plateaus of $\Delta\phi_1$. This supports the picture whereby we can think of the chaotic oscillator as making transitions between two states of locking with the phases $\phi_{1,2}$ of the competing signals.

Figures 3(b1) and 3(b2) show histogram approximations of the probability distributions of $\Delta\Phi_1 \equiv \Delta\phi_1/(2\pi)$ modulo 1 and, respectively, $\Delta\Phi_2 \equiv \Delta\phi_2/(2\pi)$ modulo 1 [16]. The purpose of these figures is to demonstrate that statistically significant correlations between ϕ and $\phi_{1,2}$ can be found. That is, each of the phases ϕ_1 and ϕ_2 weakly synchronize the chaotic attractor. [In the absence of any coupling between ϕ and $\phi_{1,2}$ these graphs would be flat, $P(\Delta\Phi_{1,2}) = 1$.]

Figures 3(c1) and 3(c2) show stroboscopic surfaces of section at the periods T_1 and, respectively, T_2. For each point on a long trajectory we plot r versus $[\phi \text{ modulo } 4\pi]/\omega_{1,2} - t$. This gives a picture of the density of the strobed points on the attractor. Both Figs. 3(c1) and 3(c2) show alternating regions of high and low density of points. (One should imagine an infinite periodic chain of such regions from which we only plotted two periods.) The high-density regions represent regions where the orbit spends a long time. The low-density regions are regions that the orbit traverses relatively faster. Therefore, the plateaus of Fig. 3(a1) [Fig. 3(a2)] correspond to regions with high density in Fig. 3(c1) [Fig. 3(c2)]. The times when ϕ slips with respect to $\phi_{1,2}$ generate regions of low density. The fact that, when Fig. 3(c1) has a low-density region, Fig. 3(c2) has a

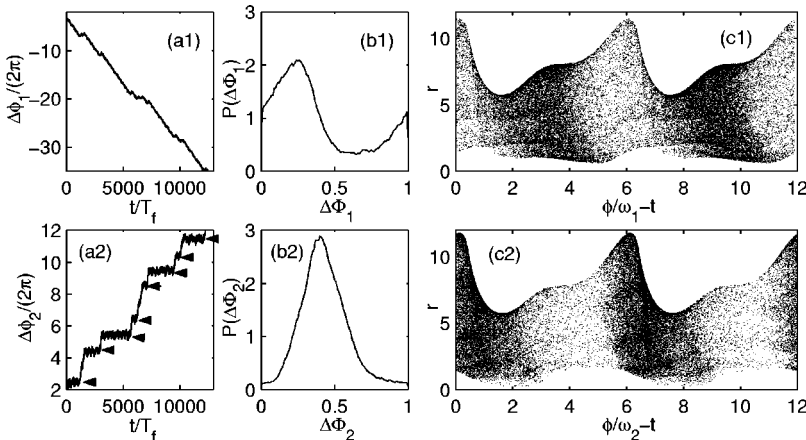FIG. 3. (a1),(a2) Difference between the geometrical phase of the attractor ϕ and the phase of the first/second sinusoidal signal $\phi_{1,2}$ versus time t/T_f. (b1),(b2) Histogram approximations of the distribution functions $P(\Delta\Phi_{1,2})$, where $\Delta\Phi_{1,2} = [\Delta\phi_{1,2}/(2\pi)]$ modulo 1. (c1), (c2) Stroboscopic sections at times $t = nT_{1,2}$ (n is an integer) through the perturbed Roessler attractor, Eqs. (1) and (2).
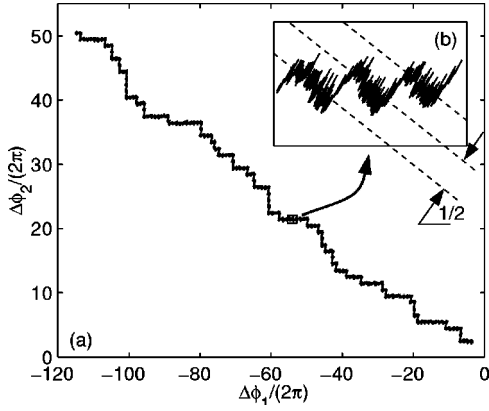
FIG. 4. (a) $\Delta\phi_2/(2\pi)$ versus $\Delta\phi_1/(2\pi)$. The staircaselike structure indicates that there are alternating time intervals in which ϕ is locked to either ϕ_1 or to ϕ_2. (b) Details of (a).

high-density region corresponds to the fact that when ϕ slips with respect to ϕ_1, it locks with respect to ϕ_2.

We now consider the possibility of phase synchronism of our system with the fast wave phase $\phi_f = \omega_f t$. Using Eq. (3), we think of $s(t)$ as a sinusoid entraining at the period T_f (the period of the fast wave) slowly modulated at the period T_s (the period of the slow wave). When the amplitude $\hat{A}$ of the fast wave becomes smaller than the threshold A_{th} set by the synchronization tongue at T_f [see Fig. 1(a)], the chaotic attractor tends [17] to lose synchronization and slip with respect to the phase of the fast wave. The synchronization condition $|\hat{A}| > A_{th}$ implies that the attractor tends to lose synchronization as $\hat{A}$ drops below A_{th} but tends to synchronize as $\hat{A}$ decreases through $-A_{th}$. Let τ denote the duration of a time interval during which $|\hat{A}| < A_{th}$ in a slow wave period T_s. If we consider the phase $\phi'(t)$ of the free running Roessler system [i.e., Eqs. (1)–(3) with $\hat{A} = 0$], then, during the time τ, the phase difference $\phi'(t) - \omega_f t$ is found to change by less than π. Thus, during a time interval τ, we expect that there is not sufficient time for $\Delta\phi_f$ to drift as much as 2π before resynchronizing after $|\hat{A}|$ exceeds A_{th}. Thus, we anticipate that slips of $\Delta\phi_f$ are solely due to the change in sign of $\hat{A}$. These slips are expected to be $\pm\pi$. In order to see this, we make a crude analogy, and consider a particle in the vicinity of a potential minimum in a sinusoidal
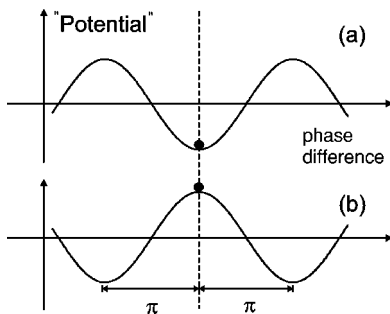

FIG. 5. Particle in sinusoidal potential: (a) at minimum potential, (b) at maximum potential after the sign change of the potential.
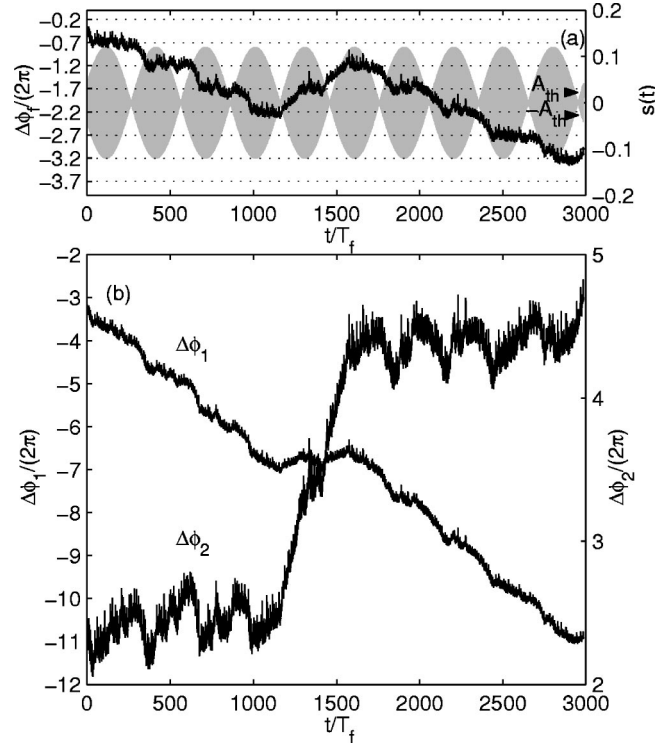

FIG. 6. (a) Detail of how $\Delta\phi_f$ switches between slipping down to slipping up with the entraining modulating slow wave indicated by the gray background. (b) Detail of how the chaotic attractor switches between locking to ϕ_2 and locking to ϕ_1. The time axes in (a) and (b) coincide.

potential [analogous to the fact that the phase $\phi(t)$ is in the vicinity of $\phi_f(t)$]; see Fig. 5(a). If we now change the sign of the potential, then the particle finds itself at the top of a potential hill, and (assuming appropriate friction) will take some time to evolve to one of the adjacent minima situated at a "phase of the potential" that is $\pm\pi$ away [Fig. 5(b)]. By these considerations, we can expect that the graph of $\Delta\phi_f$ versus time will display plateaus of synchronization and slips of π up or down occurring twice every period of the slow wave. This is illustrated in Fig. 6(a) that shows how $\Delta\phi_f$ varies with time for several periods of the slow wave. $s(t)$ is plotted as the gray background for convenience. To guide the eye, dotted horizontal lines separated by a change of π in $\Delta\phi_f$ are drawn through the plateaus.

Figure 6(b) displays $\Delta\phi_1(t)$ and $\Delta\phi_2(t)$ in the same range of time as in Fig. 6(a). Comparison of Figs. 6(a) and 6(b) reveals that time intervals of locking with the phase of the fast wave ϕ_f with π slips down correspond with the time of locking with the phase ϕ_2, while time intervals of locking with the phase of the fast wave ϕ_f with π slips up correspond with the time of locking with the phase ϕ_1. We also remark that when $\Delta\phi_f$ has a plateau, $\Delta\phi_{1,2}$ drifts slowly at the rate $\omega_f - \omega_{1,2}$ with superimposed fluctuations. During the time when $\Delta\phi_f$ slips down, $\Delta\phi_2$ may stay locked. For example, see Fig. 6(b), which shows $\Delta\phi_2/(2\pi)$ to be in a plateau for $t/T_f < 1100$. In this range, the graph of $\Delta\phi_2/(2\pi)$ versus t/T_f has a roughly sawtoothlike structure, with an upward drift with slope $(\omega_f - \omega_2)/\omega_f$ during the pla-
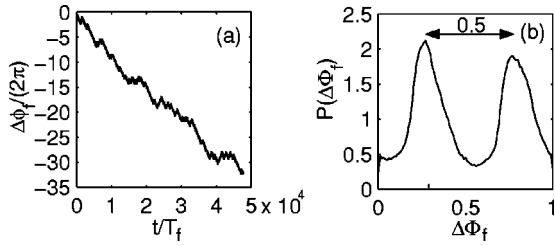
FIG. 7. (a) $\Delta\phi_f/(2\pi)$ versus time t/T_f. (b) Histogram approximation of the distribution function $P(\Delta\Phi_f)$, where $\Delta\Phi_f = [\Delta\phi_f/(2\pi)]$, modulo 1.

teaus of $\Delta\phi_f$ and rapid decrease between the plateaus of $\Delta\phi_f$.

Figure 7(a) shows $\Delta\phi_f$ over a much longer time scale than is plotted in Fig. 6(a). Refering to Fig. 4(a) and noting that $[\Delta\phi_1/(2\pi)+\Delta\phi_2/(2\pi)]/2 = \Delta\phi_f/(2\pi)$ and $[\Delta\phi_1/(2\pi)-\Delta\phi_2/(2\pi)]/2 = t/T_s$, it is seen that a $\pi/4$ rotation and a change of scale converts Fig. 4(a) to Fig. 7(a). In these coordinates [Fig. 4(a)], the jumps along the horizontal and vertical axes are integers. A close inspection of Fig. 4(a) reveals that the plateaus of $\Delta\phi_2/(2\pi)$ plotted versus $\Delta\phi_1/(2\pi)$ are not entirely flat. They have a rough sawtooth-like structure in which sawtooth segments of slope -1 correspond to the times of locking of ϕ with ϕ_f (such locking implies $\Delta\phi_1+\Delta\phi_2\sim$const). This is indicated by the blow up, Fig. 4(b), where dashed lines of slope -1 going through the plateaus of locking with ϕ_f are shown. These lines are separated by $1/2$, corresponding to the $\pm\pi$ slips in Fig. 6(a). Figure 7(b) shows a histogram approximation of the probability distribution of $\Delta\Phi_f\equiv\Delta\phi_f/(2\pi)$ modulo 1 demonstrating that the phase of the attractor ϕ weakly synchronizes with ϕ_f. The probability distribution of $\Delta\Phi_f$ in Fig. 7(b) has two maxima 0.5 apart because $\Delta\phi_f$ undergoes $\pm\pi$ jumps. This is in contrast with the probability distributions for $\Delta\phi_{1,2}$, which have only one maximum, corresponding to the fact that $\Delta\phi_{1,2}$ undergo $\mp 2\pi$ jumps, respectively.

B. Other cases

Case (ii). In this case, (A_1,T_1) is outside the single sinusoid synchronization tongue, while (A_2,T_2) and $(\hat{A},T_f)$ are inside. Histogram approximations to the distributions $P(\Delta\Phi_1)$, $P(\Delta\Phi_2)$, and $P(\Delta\Phi_f)$ (figures not included) all differ significantly from the flat distribution and look very similar to those for case (i) in Figs. 3(b1), 3(b2), and 7(b), respectively. Thus, some degree of synchronization of the chaotic system with all phases ϕ_1, ϕ_2, and ϕ_f is manifest. In addition, plots of $\Delta\phi_1$, $\Delta\phi_2$, and $\Delta\phi_f$ versus time (not included) look very similar to those in Figs. 3(a1), 3(a2), and 7(a). However, in comparison to case (i), there is significantly enhanced tendency for synchronization with phase ϕ_2 as opposed to ϕ_1. The plateaus of $\Delta\phi_2$ are longer (in average) and the plateaus of $\Delta\phi_1$ are shorter than in case (i). $\Delta\phi_f/(2\pi)$ still shows plateaus of synchronization but mostly slips up corresponding with the fact that almost all the time ϕ_2 synchronizes the orbit. At times, $\Delta\phi_f/(2\pi)$ also shows slips down, corresponding to the little bit of time the orbit spends synchronized with ϕ_1.
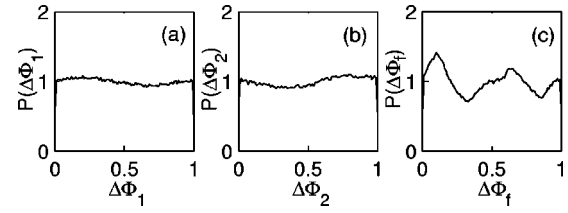

FIG. 8. Results for case (iii). (a),(b),(c) Histogram approximations of the distribution functions $P(\Delta\Phi_{1,2,f})$, where $\Delta\Phi_{1,2,f} = [\Delta\phi_{1,2,f}/(2\pi)]$ modulo 1.

Case (iii). In this case, $(A_1=A_2=A,T_f)$ lies inside the single sinusoid synchronization tongue, while (A_1,T_1) and $(\hat{A},T_f)$ are outside. Figure 8 shows histogram approximations to the distributions $P(\Delta\Phi_1)$ [Fig. 8(a)], $P(\Delta\Phi_2)$ [Fig. 8(b)], and $P(\Delta\Phi_f)$ [Fig. 8(c)]. We see that $P(\Delta\Phi_1)$ and $P(\Delta\Phi_2)$ are nearly flat, indicating very small, or negligible synchronization with phases ϕ_1 and ϕ_2. In contrast, $P(\Delta\Phi_f)$ shows two significant peaks separated by 0.5 in $\Delta\Phi_f$. This is similar to the plot of $P(\Delta\Phi_f)$ for case (i) shown in Fig. 7(b). In addition, plots of $\Delta\phi_1$ and $\Delta\phi_2$ versus time (not included) show nearly steady linear drift, while a plot of $\Delta\phi_f$ versus time (also not included) evidences periods of locking similar to Fig. 7(a) for case (i). Thus, for case (iii), we conclude that there is negligible synchronization of the system with the phases ϕ_1 and ϕ_2, but that there is significant synchronization with ϕ_f.

Case (iv). This case has only (A_2,T_2) inside the synchronization tongue, while (A_1,T_1) and $(\hat{A},T_f)$ are outside. Figures 9(b), 9(c), and 9(a), respectively, show histogram approximations to the distributions $P(\Delta\Phi_1)$, $P(\Delta\Phi_2)$, and $P(\Delta\Phi_f)$. We remark that $P(\Delta\Phi_1)$ and $P(\Delta\Phi_f)$ are almost flat, indicating little synchronization of the chaotic system with phases ϕ_1 and ϕ_f. On the other hand, $P(\Delta\Phi_2)$ shows a big peak, suggesting synchronization with phase ϕ_2. Accordingly, the graphs of $\Delta\phi_1$ [Fig. 9(a)] and $\Delta\phi_f$ versus time (not included) show nearly steady linear drift, while the graph of $\Delta\phi_2$ [Fig. 9(a)] versus time shows very long plateaus of synchronization, indicative of strong phase synchronism (see Sec. I). These results can be understood by noting that, by construction, case (iv) has (A_2,T_2) inside the single sinusoid synchronization tongue, while (A_1,T_1) and $(\hat{A},T_f)$ are outside.

Case (v). In this case we have all (A_1,T_1), (A_2,T_2), and $(\hat{A},T_f)$ outside the single sinusoid synchronization tongue. Figure 10 shows that histogram approximations to the distributions $P(\Delta\Phi_1)$ [Fig. 10(a)], $P(\Delta\Phi_2)$ [Fig. 10(b)], and $P(\Delta\Phi_f)$ [Fig. 10(c)] are all nearly flat, indicating negligible synchronization with phases ϕ_1, ϕ_2, and ϕ_f, respectively. Plots of $\Delta\phi_1$, $\Delta\phi_2$, and $\Delta\phi_f$ versus time (not included) show nearly steady linear drift. These results are not surprising since, in this case, (A_1,T_1), (A_2,T_2), and $(\hat{A},T_f)$ are far outside the single sinusoid synchronization tongue.

We have also investigated a few cases where A_1 and A_2 are unequal. For example, for the values of T_1, T_2, and $A_2 = 0.06$ used in case (i), we did computations for $A_1 = 0.01$ and $A_2 = 0.03$. In the former case, (A_1,T_1) is not in the syn-
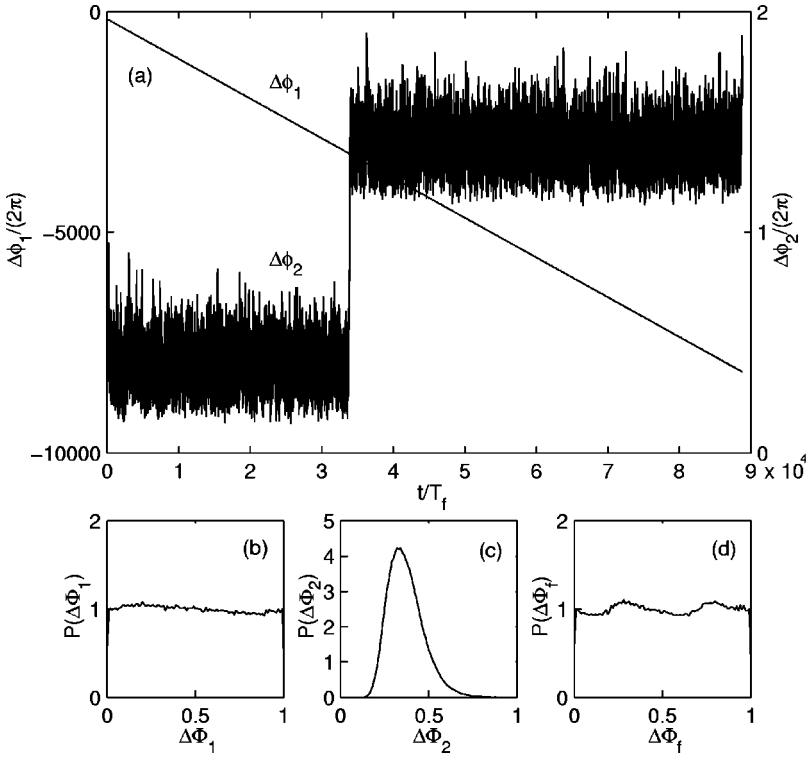
FIG. 9. Results for case (iv). (a) $\Delta\phi_1/(2\pi)$ and $\Delta\phi_2/(2\pi)$ versus time t/T_f. (b),(c),(d) Histogram approximations of the distribution functions $P(\Delta\Phi_{1,2,f})$, where $\Delta\Phi_{1,2,f}=[\Delta\phi_{1,2,f}/(2\pi)]$ modulo 1.

chronization tongue, and the phenomena observed are very similar to that in case (iv) above. In the case $A_1=0.03$ [here (A_1,T_1) is inside the synchronization tongue] we see results similar to that case (i), but with much reduced tendency for locking with phase ϕ_1.

IV. FURTHER DISCUSSIONS AND CONCLUSIONS

Even though our two frequency signal $s(t)$ is much simpler than entraining signals typically encountered in experiments [9,12], we believe that it offers an important lesson regarding the understanding of synchronization by entrainers with complicated continuous frequency spectra. Data analysis of numerical and experimental results [8,9,12] shows that one can assign a phase to a signal (for the purpose of detecting phase synchronization of chaotic systems) by either bandpass filtering or by the use of the Hilbert transform. It has been found in experiments that the detection of phase synchronism can be enhanced by bandpass filtering [9,12]. If we were to apply a bandpass filter to our two frequency
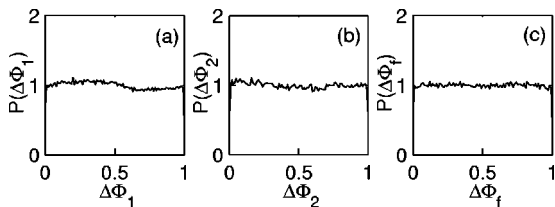

FIG. 10. Results for case (v). (a),(b),(c) Histogram approximations of the distribution functions $P(\Delta\Phi_{1,2,f})$, where $\Delta\Phi_{1,2,f}=[\Delta\phi_{1,2,f}/(2\pi)]$ modulo 1.

signal $s(t)$, then, assuming a filter bandwidth less than $(\omega_1-\omega_2)$, we would pick either the sinusoid at ω_1 or the sinusoid at ω_2, depending on the center frequency of the bandpass filter. Thus the phase of the filtered signal would be either ϕ_1 or ϕ_2. Alternatively, consider the case where we do no filtering and use the Hilbert transform technique, as advocated in Ref. [8], to produce $\tilde{s}(t)$, the complex "analytic signal" corresponding to $s(t)$. This yields

$$\tilde{s}(t)=A_1\exp(i\omega_1 t)+A_2\exp(i\omega_2 t).$$

The associated "Hilbert phase," ϕ_H, is

$$\tan\phi_H=\frac{\mathrm{Im}[\tilde{s}(t)]}{\mathrm{Re}[\tilde{s}(t)]}=\frac{A_1\sin(\omega_1 t)+A_2\sin(\omega_2 t)}{A_1\cos(\omega_1 t)+A_2\cos(\omega_2 t)}.$$

For $A_1=A_2$, this gives $\tan\phi_H=\tan[(\omega_1+\omega_2)t/2]$, or $\phi_H=\phi_f$ [18]. Thus by filtering we obtain ϕ_1 or ϕ_2, while by not filtering and using the Hilbert phase we obtain ϕ_f (for $A_1=A_2$). Which procedure is best? The answer to this question depends on circumstances. For example, in our cases (i), (ii), and (iv) synchronism with $\phi_2(t)$ is strong and clearly manifest; if a continuous spectrum had such a case, filtering might be thought to clean up the phase and make phase synchronism more apparent (as indeed has been found in some experiments [9,12]). If, however, the situation is more like that of case (iii), where the only detectable synchronism is with ϕ_f, then narrow bandpass filtering (which yields

ϕ_1 or ϕ_2) would not reveal any synchronism, while applying the Hilbert transform to the unfiltered signal would reveal synchronism.

In conclusion, in this paper we have investigated the situation in which two sinusoidal signals compete to phase synchronize a chaotic oscillator. We find and illustrate several possible outcomes of this situation.

(1) Phase synchronism can be discerned to be present to some degree for both sinusoids as well as for the mean phase of the sinusoids, ϕ_f [cases (i) and (ii)].

(2) Phase synchronism can be discernable only for the mean phase [case (iii)].

(3) Phase synchronism is discernable only for one of the sinusoids [case (iv)].

---

[1] A. S. Pikovsky, Sov. J. Commun. Technol. Electron. **30**, 85 (1985).

[2] E. F. Stone, Phys. Lett. A **163**, 367 (1992).

[3] A. Pikovsky, G. Osipov, M. Rosenblum, M. Zaks, and J. Kurths, Phys. Rev. Lett. **79**, 47 (1997).

[4] E. Rosa, E. Ott, and M. H. Hess, Phys. Rev. Lett. **80**, 1642 (1998).

[5] M. A. Zaks, E.-H. Park, M. G. Rosenblum, and J. Kurths, Phys. Rev. Lett. **82**, 4228 (1999).

[6] C. M. Ticos, E. Rosa, W. B. Pardo, J. A. Walkenstein, and M. Monti, Phys. Rev. Lett. **85**, 2929 (2000).

[7] E. Allaria, F. T. Arecchi, A. Digarbo, and R. Meucci, Phys. Rev. Lett. **86**, 791 (2001).

[8] M. G. Rosenblum, A. S. Pikovsky, and J. Kurths, Phys. Rev. Lett. **76**, 1804 (1996).

[9] P. Tass, M. G. Rosenblum, J. Weule, J. Kurths, A. Pikovsky, J. Volkmann, A. Schnitzler, and H.-J. Freund, Phys. Rev. Lett. **81**, 3291 (1998).

[10] F. Mormann, K. Lehnertz, P. David, and C. E. Elger, Physica D **144**, 358 (2000).

[11] A. Stefanovska, H. Haken, P. V. E. McClintock, M. Hožič, F. Bajrović, and S. Ribarič, Phys. Rev. Lett. **85**, 4831 (2000).

[12] D. J. DeShazer, R. Breban, E. Ott, and R. Roy, Phys. Rev. Lett. **87**, 044101 (2001).

[13] D. Maza, A. Vallone, H. Mancini, and S. Boccaletti, Phys. Rev. Lett. **85**, 5567 (2000).

[14] O. Roessler, Phys. Lett. **57A**, 397 (1976).

[15] The parameter σ governs the amount of enhanced dispersion of the orbit circulation times. The chosen value $\sigma=0.002$ is the same as that used in Ref. [4], and as can be seen from Fig. 2 of that reference, the added dispersion significantly affects the synchronization tongue in the vicinity of the chosen value of A ($A=0.06$).

[16] The length of the time series used to build the histogram graphs is four times larger than the length of the time series shown in Figs. 3(a1) and 3(a2), respectively. All histograms in this work have the same number of sample points distributed over 100 bins, which makes an average of 2850 points/bin, ensuring good statistics for our purpose. (The expected percentage error for a typical bin is of the order of $100/\sqrt{2850} \approx 2\%$.)

[17] In this regard, we note that Fig. 1(a) only shows the region of locking parameters (A_0,T) in the limit of $t\rightarrow\infty$. Transients are not reflected by this figure. Thus, one should not expect that the slips occur exactly when $|\hat{A}|$ drops below A_{th}. Furthermore, the tongue of significant weak synchronization is larger than the one for perfect synchronization displayed in Fig. 1(a).

[18] When $A_1 \gg A_2$, $\phi_H(t) \sim \phi_1(t)$ and when $A_2 \ll A_1$, $\phi_H(t) \sim \phi_2(t)$.